Organisms Diversity & Evolution
https://doi.org/10.1007/s13127-019-00410-6

ORIGINAL ARTICLE

Phylogenetic relationships within the flatworm genus *Matuxia* (Platyhelminthes, Tricladida, Continenticola) inferred from molecular data with the description of a southern lineage of the genus

Ilana Rossi[1,2,3] · Silvana Vargas do Amaral[1,2] · Giovana Gamino Ribeiro[4] · Mário Josias Müller[4] · Victor Hugo Valiati[1,4] · Ana Maria Leal-Zanchet[1,2]

Received: 18 March 2019 / Accepted: 25 July 2019

Abstract

The genus *Matuxia* Carbayo et al., 2013 currently comprises two species with distribution restricted to southeastern Brazil. In the present study, based on an integrative approach, we examine the genetic diversity within the genus and describe a new species, *Matuxia tymbyra* Rossi and Leal-Zanchet, sp. nov., representing a southern lineage of the genus. We employed one mitochondrial (cytochrome c oxidase subunit I, COI) and other nuclear (elongation factor 1a, EF-1a) markers to investigate the phylogenetic relationships within the genus. Maximum-parsimony analysis in a segment of the COI gene of 676 nucleotides showed 79 (11.68%) nucleotide positions exhibiting autapomorphic characters that support the occurrence of three independent evolutionary molecular operational taxonomic units in the genus. Similar evaluation for the dataset of the EF-1a gene showed a much smaller number of autapomorphies. Bayesian inference, maximum-likelihood and delimitation approaches, based on evolutionary models, showed that *M. tymbyra* is the sister species of the type-species of the genus, *Matuxia tuxaua*. They should be considered sibling species, only distinguishable based on details regarding eye arrangement and prostatic vesicle. The existence of 15 and 23 molecular autapomorphies, as revealed by maximum-parsimony analysis in a segment of the COI gene for *M. tymbyra* and *M. tuxaua*, respectively, allowed us to propose a molecular diagnosis for the new species, which is essential in cases of sibling species. The new species seems to be endemic from areas of *Araucaria* Forest in southern Brazil; the record augments the known distribution of the genus to the south.

Keywords Geoplaninae · Triclads · Taxonomy · Atlantic forest · Neotropical region · Sibling species

Introduction

The genus *Matuxia* Carbayo et al., 2013 currently comprises two species with distribution restricted to southeastern Brazil, in areas of dense ombrophilous forest (Atlantic Forest): *Matuxia tuxaua* (E.M. Froehlich, 1955) and *Matuxia matuta* (E.M. Froehlich, 1955) (Froehlich 1955b; Carbayo et al. 2013). Both species show a similar pigmentation and eye patterns and present a homogeneous copulatory apparatus, being differentiated by details of the female copulatory organs. During surveys in areas of the southern portion of the Brazilian Atlantic Forest (mixed ombrophilous forest or *Araucaria* forest), we found a southern lineage of *Matuxia* (Leal-Zanchet & Carbayo 2000; Leal-Zanchet and Baptista 2009; Leal-Zanchet et al. 2011), which is almost morphologically indistinguishable from *M. tuxaua*.

Among land flatworms, species presenting similar external features, but being distinguished by a combination of details of the reproductive system and pharyngeal anatomy, constitute a common event (Lemos et al. 2014; Carbayo et al. 2017; Amaral et al. 2018a). Sometimes, however, it is so difficult to know whether we are dealing with specific differences or population variations that the use of an integrative taxonomy

Electronic supplementary material The online version of this article (https://doi.org/10.1007/s13127-019-00410-6) contains supplementary material, which is available to authorized users.

✉ Ana Maria Leal-Zanchet
zanchet@unisinos.br

[1] Programa de Pós-Graduação em Biologia, Universidade do Vale do Rio dos Sinos – UNISINOS, São Leopoldo, RS 93022-000, Brazil

[2] Instituto de Pesquisas de Planárias, Universidade do Vale do Rio dos Sinos – UNISINOS, São Leopoldo, RS 93022-000, Brazil

[3] Instituto Federal de Educação, Ciência e Tecnologia do Rio Grande do Sul - Campus Vacaria, Vacaria, RS 95200-000, Brazil

[4] Laboratório de Genética e Biologia Molecular, Universidade do Vale do Rio dos Sinos – UNISINOS, São Leopoldo, RS 93022-000, Brazil

Published online: 06 August 2019

combining molecular data with morphological analyses is necessary (Amaral et al. 2018b). Molecular phylogenetic analyses may be useful to reveal many genetically distinct lineages in one apparently morphologically uniform unit, thus helping to differentiate species (Frankham et al. 2012; Álvarez-Presas et al. 2015). When two or more species are morphologically indistinguishable, they have been considered cryptic species. Yet the term sibling connotes more recent common ancestry than does the word cryptic, thus indicating a sister-species relationship (Saez and Lozano 2005; Bickford et al. 2007).

Hence, aiming to investigate whether external features, as well as anatomical characters of the reproductive system constitute intra- or inter-specific variations within *Matuxia*, we use molecular data based on two markers combined with anatomical and histological information. Considering that we found strictly similar characters between *M. tuxaua* and the southern specimens of *Matuxia*, we asked (1) does this southern lineage represent a different species of *Matuxia*? (2) if so, do *M. tuxaua* and this southern lineage present a sister-group relationship, constituting sibling species? and (3) what is the basal clade within *Matuxia*?

Material and methods

Specimens of *M. tymbyra* Rossi and Leal-Zanchet, sp. nov. were collected from two protected areas, São Francisco de Paula National Forest (29°23′–29°27′S; 50°23′–50°25 W) and Research and Conservation Center Pró-Mata (29°28′–29°31′S; 50°08′–50°14′W), both located in São Francisco de Paula, state of Rio Grande do Sul, Brazil (Fig. 1). Sampling took place between May 1998 and August 2013 mainly in areas of Mixed Ombrophilous Forest and in plantations of the native *Araucaria angustifolia* (Bertol.) O. Kuntze. Specimens were collected during the day by direct sampling in leaf litter and under fallen logs and stones, many of them partially buried. The specimens collected, locality data, and GenBank accession numbers are listed in Supplementary Table S1.

Morphological analysis

Live specimens were analysed regarding colour pattern and body shape and dimensions. Before fixation, the posterior tip of five specimens was cut and preserved in 100% ethyl alcohol for molecular analysis. After that, specimens were killed by pouring boiling water over them. Specimens were then fixed in neutral formalin 10% and subsequently maintained in 70% ethyl alcohol. Characteristics of the external morphology, such as colour pattern, body length and width, mouth and gonopore position and distribution of eyes, were analysed under stereomicroscope. The analysis of eye arrangement was also done after immersion of a fixed specimen in clove oil for 96 h.

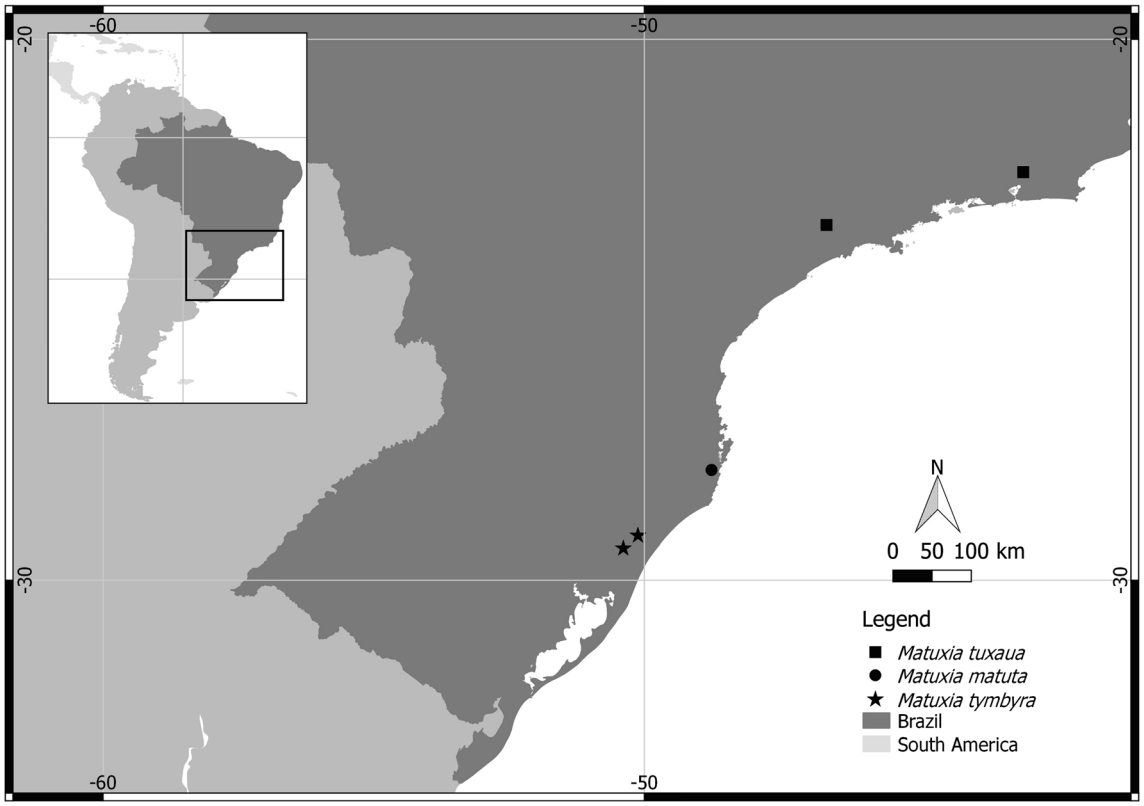

Fig. 1 Distributional range of the genus *Matuxia* in areas of Atlantic Forest from southeastern and southern Brazil

Body fragments, namely the anterior tip, the subsequent body region containing ovaries, a pre-pharyngeal region and the body regions containing the pharynx and the copulatory apparatus, were cut, dehydrated in an ascending ethyl alcohol series, cleared in isopropyl alcohol and embedded in paraplast. Histological sections at 6 μm were stained with haematoxyline/eosine or Goldner's Masson trichrome (Romeis 1989).

The ratio of the height of the cutaneous musculature to the height of the body (mc:h index in Froehlich 1955a) was determined in the median region of a transverse section of the pre-pharyngeal region. Mesenchymal muscle fibres were counted in transverse sections of the same region.

Type-material was deposited in the following reference collections: Museu de Zoologia da Universidade do Vale do Rio dos Sinos, São Leopoldo, Rio Grande do Sul, Brazil (MZU), and the Helminthological Collection of Museu de Zoologia da Universidade de São Paulo, São Paulo, state of São Paulo, Brazil (MZUSP).

DNA extraction, PCR amplification and sequencing

The Wizard® Genomic DNA Purification Kit (Promega, Madison, WI, USA) was used to extract Genomic DNA from the specimens of *Matuxia* preserved in 100% ethyl alcohol. Two molecular markers were amplified, sequenced and analysed: (1) partial sequences of the mitochondrial COI gene using the primer pairs BarT (Álvarez-Presas et al. 2011) and COIR (Lázaro et al. 2009), and (2) a region of the nuclear gene elongation factor 1-alpha (EF-1a) using primers EFplatF and EFplatR (Carbayo et al. 2013). Details of amplification reactions and PCR cycling profiles can be seen in Supplementary Table S2. Prior to sequencing, PCR products were purified using Shrimp Alkaline Phosphatase (SAP) and exonuclease I (New England Biolabs), following the manufacturer's recommendation. The purified amplicons from COI and EF-1a were submitted to direct sequencing at Macrogen (Macrogen Inc., Seoul, Korea), and each sample was sequenced in both directions.

Sequence and phylogenetic analyses

We visually inspected the chromatogram quality in Chromas Pro 1.5 software (http://www.technelysium.com.au). Sequences were also checked using the BLASTn on-line tool for comparison with sequences deposited in the GenBank database (NCBI). Sequences were aligned separately and as a combined matrix (concatenated sequences of both genes), using ClustalX Sofware 2.0.9 (Thompson et al. 1997) and inspected visually for poorly aligned sites using BioEdit 5.0.9 (Hall 1999). They were checked for unexpected frameshift mutations or stop codons in MEGA 6 (Tamura et al. 2013). The best-fit model of sequence evolution for each alignment (COI, EF-1a, combined matrix) was inferred according to the Akaike information criterion (AIC) (Akaike 1974) using the jModelTest 2.1.1 software (Darriba et al. 2012). Phylogenetic trees were constructed using a combined matrix of genes (concatenated COI + EF-1a) and were conducted using maximum likelihood (ML) with RAxML (Stamatakis 2006) and Bayesian inference (BI) using MrBayes (Ronquist et al. 2012). The model of sequence evolution was GTR+I+G (−lnL = 4405.8633) for the COI and the GTR+ G (−lnL = 2190.3625) for EF-1a. For the concatenated dataset, we assumed the same priors as for the individual gene analyses for each partition.

The ML tree was conducted with a heuristic search to find the most probable topologies based on the substitution models; statistical support for the likelihood hypothesis was evaluated by bootstrap analysis with 1000 pseudo-replications (Felsenstein 1985). We consider bootstrap values of ≥ 70% as strongly supported (Hillis and Bull 1993). For Bayesian analyses, we used the optimal model determined and the default priors; three heated and one cold Markov chains were run from two random starting points. We ran the Markov chain Monte Carlo search with 10 million generations (repeated three times), with a random starting tree, and sampled every 1000 generations; the first 25% trees were discarded as "burn-in." At that point, the chain reaches a stationary state; this ensures that the average split frequency between the runs is less than 1%. We considered as statistically well-supported values posterior probabilities > 0.95 (PP). We estimated the distance pairwise nucleotide distances by Kimura's two-parameter (Kimura 1980), between all sequences with 1000 bootstrap replications in the programme MEGA version 6 (Tamura et al. 2013). We use PAUP* version. 4.0b10 (Swofford 2002) to determine the molecular autapomorphies for the dataset of the two genes and calculate the consistency index and retention index of each character using heuristic parsimony analysis, with 100 random stepwise additions of taxa (tree bisection–reconnection branch swapping) under ACCTRAN and DELTRAN optimisation.

The molecular operational taxonomic unit (MOTU)

In the present study, we used as dataset a combined matrix of genes (concatenated COI + EF-1a), and two evolutionary model-based methods for delimiting the number the putative species: (i) the Generalized Mixed Yule Coalescent (GMYC) method for delimiting species (Fujisawa and Barraclough 2013) and (ii) the Poisson Tree Processes (PTP) model (Zhang et al. 2013). The single threshold GMYC method was implemented in the R package "splits" (SPecies LImits by Threshold Statistics) (Monaghan et al. 2009). We used the unique threshold method to detect the transition point between intra- and inter-specific relationships, based on the length of the branches (Pons et al. 2006). An ultrametric tree was

generated in the BEAST v.2.2.1 package (Bouckaert et al. 2014) from the combined matrix of genes and used as input into the GMYC analysis. The parameters estimated in the jModelTest were used in the BEAUti programme assuming a relaxed molecular clock with a lognormal distribution and Yule model. Three independent runs were carried out in BEAST 2 with 4×10^7 generations each. Later, the effective sample size (ESS > 200) of each run was verified in Tracer v1.5 (Rambaut and Drummond 2009). The TreeAnnotator software was used to summarize the information from a sample of trees (30% burn-in percentage, 0.5 posterior probability limit and mean heights node) onto a maximum clade credibility tree. The PTP model was based on our inferred molecular phylogeny. The maximum likelihood using RAxML (Stamatakis 2006) was employed as input data to PTP. The calculations for PTP were conducted on the bPTP webserver (http://species.h-its.org/ptp/), with default settings. The corresponding analyses were carried out using trees with the maximum likelihood solution from the ML analyses and the majority-rule consensus topology resulting from the BI analyses.

The molecular diagnosis of the new species includes the nine specimens shown in the Supplementary Table S1. We used as dataset a combined matrix of genes (concatenated COI + EF-1a) in phylogenetic analyses and delimitation tools.

Abbreviations used in the figures

(ca) copulatory apparatus; (cg) cyanophil glands; (cmc) common muscle coat; (cov) common glandular ovovitelline duct; (cs) creeping sole; (de) dorsal epidermis; (df) dorsal fold; (di) dorsal insertion; (dm) dorsal cutaneous musculature; (dsm) dorsal subcutaneous mesenchymatic musculature; (dvm) dorso-ventral mesenchymatic musculature; (e) eye; (ec) ejaculatory cavity; (eg) erythrophil glands; (fa) female atrium; (fc) female canal; (go) gonopore; (i) intestine; (im) internal musculature; (lu) pharyngeal lumen; (m) mouth; (ma) male atrium; (ms) median stripe; (n) nerve cord; (o) ovary; (oe) oesophagus; (om) outer musculature; (ov) ovovitelline ducts; (p) penis papilla; (ph) pharynx; (pp) pharyngeal pouch; (pv) prostatic vesicle; (rg) rhabditogen glands; (sbm) sub-intestinal transverse mesenchymatic musculature; (sg) shell glands; (sp) sensory pit; (spm) supra-intestinal transverse mesenchymatic musculature; (sv) spermiducal vesicle; (t) testes; (v) vitellaria; (vi) ventral insertion; (vm) ventral cutaneous musculature; (xg) xanthophil glands.

Results

Molecular results

The sequences aligned did not show insertions, deletions, NUMTs (nuclear DNA sequences originating from mitochondrial DNA sequences) or stop codons. We detected 194 (27.8%) variable nucleotide sites in the COI gene (out of a total of 700 bp nucleotide sites included in the analyses). We obtained an intraspecific K2P distance of 0.03% for nine specimens of the southern clade, whereas the intraspecific K2P mean distances for all species were less than 2% (Supplementary Fig. S1A). Based on our data, the lowest interspecific genetic distance was observed between the specimens of *Matuxia tuxaua* and the new species herein described as *Matuxia tymbyra* Rossi and Leal-Zanchet, sp. nov. (7.3%), whereas the genetic distance between *Matuxia matuta* and *M. tymbyra* was 10.1%. The average distance between all genera was > 14% (14.1 to 16.9%). EF-1a gene reveal 128 (23%) variable nucleotide sites in the total of 556 bp analysed. Using the K2P parameter in all possible pairwise comparisons, we found an average intraspecific distance of 1.30%, while the interspecific distance was of 6.41% on average (Supplementary Fig. S1B). The five specimens of *M. tymbyra* analysed for this gene did not present nucleotide differences in their 556 bp. The distribution of K2P pairwise differences can be seen in the Supplementary Fig. S1A and B, with the shortest distances (black bars) representing the intraspecific comparisons, while the higher distances (grey bars) interspecific divergence.

The concatenated data matrix of the two genes included 1499 characters and 19 taxa. Both the ML and the BI analyses recovered well-supported relationships (bootstrap > 90% and posterior probabilities (PP) = 98) between species of *Matuxia*, as well as confirmed that the species herein studied is closely related to *M. tuxaua* (Fig. 2).

Molecular autapomorphies of species of *Matuxia* as revealed by maximum-parsimony analysis in a segment of the COI gene of 676 nucleotides showed 79 (11.68%) nucleotide positions exhibiting autapomorphic characters that support the condition of three independent species for the genus *Matuxia*. The new species *M. tymbyra* showed 15 autapomorphies; *M. tuxaua* 23 and *M. matuta* 41 (see Supplementary Table S3). A similar evaluation for the dataset of the EF-1a gene showed a much smaller number of autapomorphies. For a segment of 556 nucleotides, 18 (3.24%) constituted autapomorphic characters. *Matuxia tymbyra* and *M. tuxaua* showed three autapomorphies each, while *M. matuta*, the basal species of the genus, showed 12 autapomorphic sites (see Supplementary Table S4).

In total, 19 individuals from nine recognized species of four genera and the new species were tested for molecular delimiters of species using a concatenated data matrix. The maximum likelihood of the null model ($\log L_{NULL} = 79.75599$), in which all sequences belong to a single species, was significantly lower than the maximum likelihood of the GMYC model ($\log L_{GMYC} = 88.2272$) (p value < 0.001), indicating that the number of putative species and MOTUs is ten and the species herein described corresponds to a new evolutionary lineage of *Matuxia* (Fig. 2). For the single phylogenetic tree, based on the best-fit ML, PTP

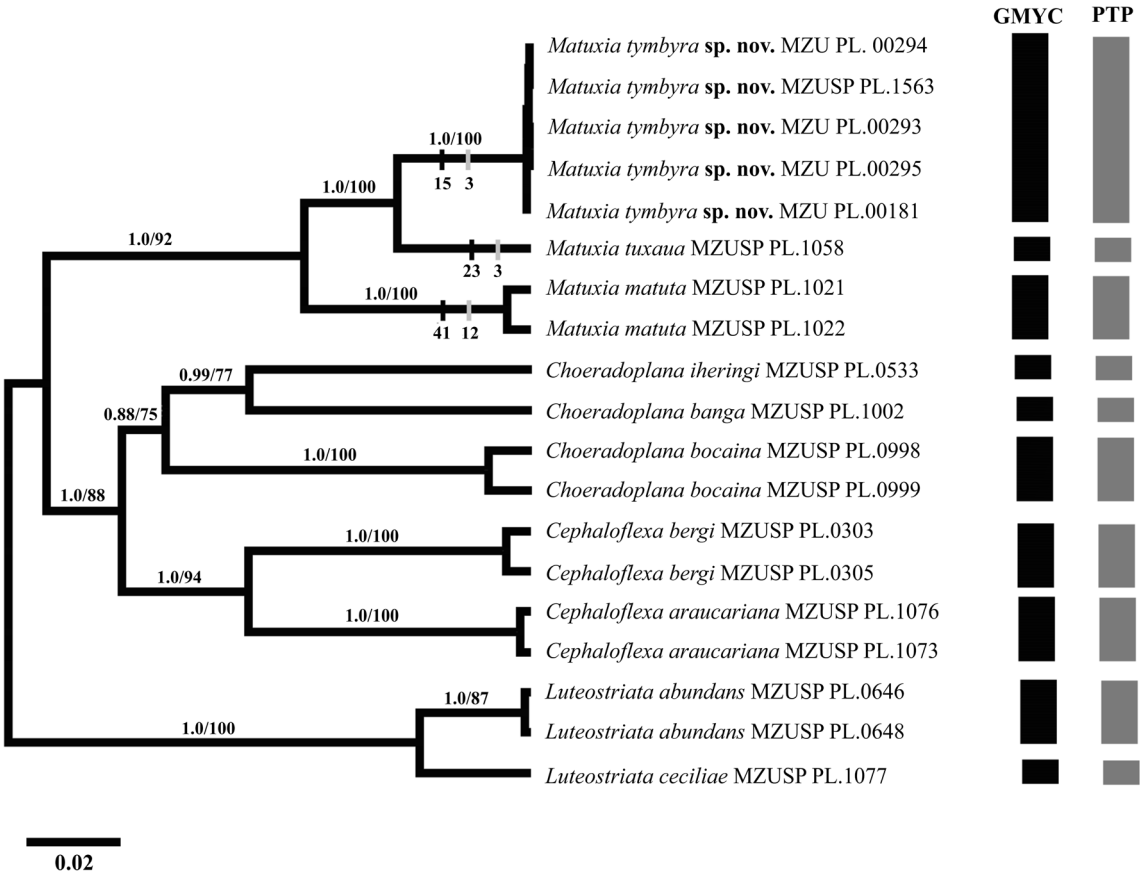

Fig. 2 Molecular phylogenetic relationships and species boundaries inferred from the sequences of COI and EF-1a on a Bayesian consensus tree. Node values represent posterior probabilities and likelihood bootstrap, respectively. The number of autapomorphies for each species of *Matuxia* is shown below the branches; bars indicate the genes (black bar COI gene and grey for EF-1a)

estimated 10 species from a dataset of 19 specimens (Fig. 2). All clusters under both PTP model formed monophyletic clades with high node bootstrap supports (> 0.80).

Taxonomic part

Family Geoplanidae.

Subfamily Geoplaninae.

Matuxia Carbayo et al., 2013

Matuxia tymbyra Rossi and Leal-Zanchet, sp. nov.

Geoplana sp. 4: Leal-Zanchet and Carbayo 2000.

Geoplana sp. 2: Leal-Zanchet and Baptista 2009.

Geoplana sp. 2: Leal-Zanchet, Baptista, Campos and Raffo 2011.

Etymology

The specific name, from tupi, means buried and refers to the fact that type-specimens were mainly found buried into the soil.

Material examined

Holotype: MZUSP PL.1563: *I. Rossi*, *coll.* 08. August 2013: São Francisco de Paula (São Francisco de Paula National Forest), RS, Brazil — anterior tip: transverse sections on 47 slides; pre-pharyngeal region: transverse sections on 17 slides; pharynx: sagittal sections on 24 slides; copulatory apparatus: sagittal sections on 15 slides.

Other specimens: MZU PL.00180: L. Teixeira, *coll.* 31. May 1998: São Francisco de Paula (São Francisco de Paula National Forest), RS, Brazil — anterior region in two fragments: sagittal sections on 16 slides and transverse sections on 58 slides; pre-pharyngeal region: transverse sections on five slides; pharynx: sagittal sections on 14 slides; copulatory apparatus: sagittal sections on 24 slides. MZU PL.00181: I. Rossi, *coll*. 30. July 2013: São Francisco de Paula (São Francisco de Paula National Forest), RS, Brazil — copulatory apparatus: sagittal sections on 26 slides. MZU PL.00182: N. Zanchet, *coll*. 25. October 2003: São Francisco de Paula (Research and Conservation Center Pró-Mata), RS, Brazil — pre-pharyngeal region: transverse sections on five slides; pharynx: sagittal sections on 18 slides; copulatory apparatus: sagittal sections on 17 slides. MZU PL.00183: V. A. Baptista, *coll*. 08. September 2000: São Francisco de Paula (São Francisco de Paula National Forest), RS, Brazil — copulatory apparatus: sagittal sections on 20 slides. MZU PL.00166: P. K. Boll, *coll.* 15. September 2010: São Francisco de Paula (São

Francisco de Paula National Forest), RS, Brazil — copulatory apparatus: horizontal sections on 17 slides.

Type-locality: São Francisco de Paula (São Francisco de Paula National Forest), state of Rio Grande do Sul (RS), Brazil.

Distribution: Rio Grande do Sul (São Francisco de Paula), Brazil.

Diagnosis: greyish dorsal surface with light thin median stripe and light body margins; marginal eyes in one-to-two series, without clear halos; glandular margin absent; *mc:h* 12%–14%; anterior-most testes at the same level as ovaries; ovaries pyramidal and lobated; ovovitelline ducts emerging ventrally, but laterally displaced, from the anterior or median third of ovaries, and ascending approximately at the level of the gonopore; male atrium entirely occupied by a conical and asymmetrical penis papilla; male and female atria separated by a dorsal fold. Molecular diagnosis: this species includes all populations that cluster with specimens MZU PL.00181 to MZU PL.00294 with significant support in phylogenetic analyses and show the following molecular autapomorphies determined for each gene: COI gene, G(19), G(27), A(45), T(72), G(105), A(207), A(213), G(309), A(363), A(366), G(372), G(402), T(498), A(528), and A(642); EF-1a gene, C(270), G(420) and T(555).

Description

External features

Body elongate with parallel margins, anterior tip rounded and posterior tip pointed (Fig. 3a–b). In maximal extension, length reaches 88 mm in the holotype (Table 1). When creeping, the cephalic region appears much narrower than the rest of the body. At rest, body height is much larger than when creeping, with waved body margins. Mouth and gonopore located approximately in the posterior fourth of the body (Table 1, see Fig. 3c).

Alive, dark-grey dorsum with light-grey margins, sometimes slightly pinkish (Fig. 3a–b). Under the stereomicroscope, light-grey dorsal ground-colour also visible on a thin

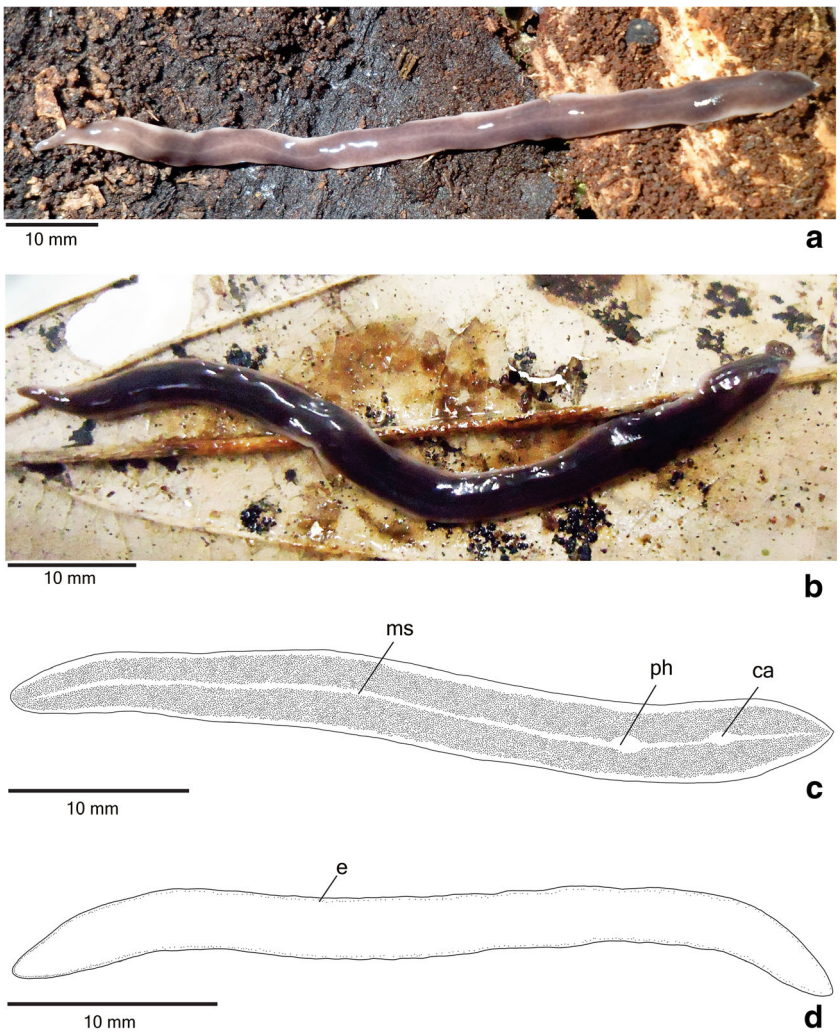

Fig. 3 *Matuxia tymbyra* Rossi & Leal-Zanchet, sp. nov.: **a**–**b** photograph of live specimens, **a** MZU PL.00181 and **b** holotype, in dorsal view; **c** colour pattern of the holotype after fixation in dorsal view; **d** eye pattern of a fixed specimen (MZU PL.00183) in dorsal view. Anterior tip to the left. The position of the pharynx and copulatory apparatus is indicated by the light marks on dorsal surface in **c**

Table 1 Measurements, in mm, of specimens of *Matuxia tymbyra* Rossi & Leal-Zanchet, sp. nov.

	Holotype MZUSP PL.1563	Specimen MZU PL. 00180	Specimen MZU PL. 00181	Specimen MZU PL. 00182	Specimen MZU PL. 00183	Specimen MZU PL. 00166
Maximum length in extension	88	65	81	70	–	75
Maximum width in extension	2	2	3	2.5	–	3
Length at rest	50	20	37	40	60	50
Width at rest	3	5	4.5	4	2	4
Length*	43	35	54.5	56	38	39
Width*	4	4	4	3	2.5	6
DM*	31 (72)	25 (71.5)	40 (73.5)	42 (75)	27 (71)	30 (77)
DG*	35 (81.5)	30 (86)	46 (84.5)	51 (91)	32 (84)	35 (90)
DMG*	4	5	6	9	6	5
DPVP	2.1	2.3	–	2.6	–	–
Ovaries	8 (18.5)	6.5 (18.5)	–	–	–	–
Anteriormost testes	8.2 (19)	6.5 (18.5)	–	–	–	–
Posteriormost testes	29.5 (70)	22 (63)	–	–	–	–
Prostatic vesicle**	1.0	0.5	1.1	0.9	0.8	1.0
Penis papilla**	1.4	0.8	1.6	1.8	1.4	0.8
Male atrium**	1.8	1.0	2	2.4	1.9	1.1
Female atrium**	1.4	0.9	1.6	1.3	1	1.3

–: not measured; *: After fixation; **: length; DG: distance of gonopore from anterior end; DM: distance of mouth from anterior end; DMG: distance between mouth and gonopore; DPVP: distance between prostatic vesicle and pharyngeal pouch. The numbers given in parentheses represent the position relative to body length

median stripe, besides body margins (Fig. 3c). The remaining dorsal surface covered by thin and dense distributed dark-grey pigmentation. Ventral surface light-grey with dark-grey anterior tip. Specimen MZU PL.00182 shows ventral surface and dorsal ground-colour pinkish. After fixation, dorsal and ventral colour fades, dorsal ground-colour and ventral surface becoming whitish. Median stripe with maximum width of 0.25 mm (7% of the body width) in the holotype, becoming narrower towards anterior and posterior tips (Fig. 3c).

Eyes, initially uniserial and with pigment cups of about 20 μm in diameter, surround anterior tip. After the second millimetre, they are mixed with larger eyes (eye cups of 30 μm in diameter). They are monolobated and remain marginal along body length (Fig. 3d), but form an irregular series in the median body third. Eyes become less numerous towards the posterior tip. Clear halos are absent.

Sensory organs, epidermis and body musculatures

Sensory pits (Fig. 4a–b) occur as simple invaginations ventromarginally in an irregular row in the anterior 1/8th of the body. Their depth is about 20 to 30 μm.

Creeping sole occupying the whole body width (Table 2). Three types of glands discharge through the entire epidermis of the pre-pharyngeal region, without forming a glandular margin (Fig. 4c): numerous rhabditogen cells with xanthophil secretion (rhammites); cells with amorphous cyanophil secretion, sometimes with a coarse granular appearance, and scarcer glands with granular erythrophil secretion. Openings from cyanophil glands with amorphous secretion are more numerous through the creeping sole. Cell bodies from rhabditogen glands aggregate on body margins (Fig. 4c) and their openings are abundant through dorsal epidermis and body margins. On the anterior tip, openings from rhabditogen cells are more numerous through the creeping sole than through the dorsal epidermis and body margins, with cell bodies concentrating beneath the ventral cutaneous musculature; other glands are similar to those of the pre-pharyngeal region (Fig. 4a–b).

Cutaneous musculature with the usual three layers: circular, oblique and longitudinal layers; longitudinal layer with thick bundles (Fig. 4d–e, Table 2). Musculature thicker laterally than medially, but becoming progressively thinner close to body margins; ventral musculature thicker

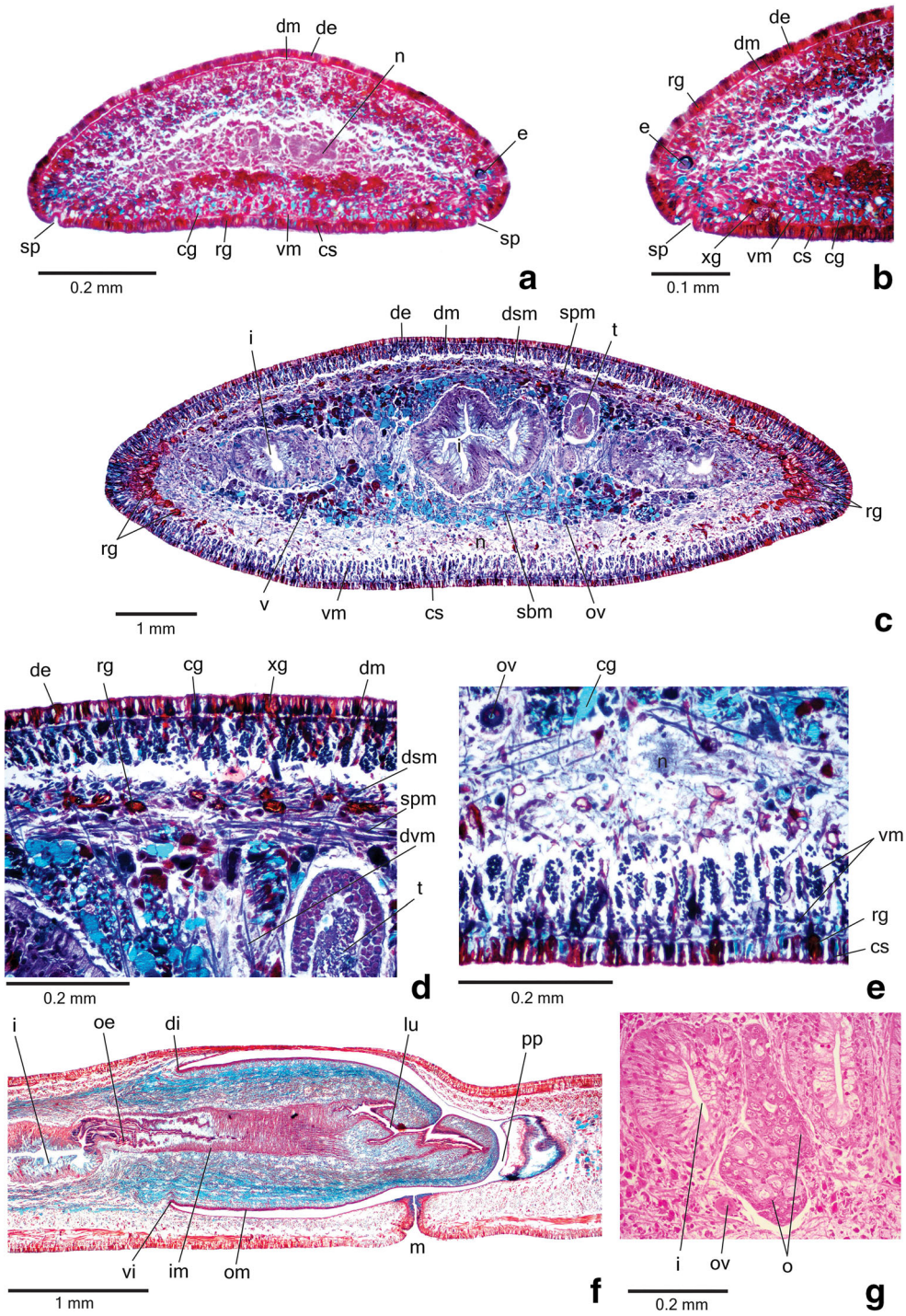

Fig. 4 *Matuxia tymbyra* Rossi & Leal-Zanchet, sp. nov., holotype, microphotographs of transverse (**a**–**e**, **g**) and sagittal (**f**; anterior tip to the left) sections: **a** anterior region of body; **b** detail of anterior region of body; **c** pre-pharyngeal region; **d** detail of dorsal surface of pre-pharyngeal region; **e** detail of ventral surface of pre-pharyngeal region; **f** pharynx; **g** ovary

than dorsal at the sagittal plane, being between about three times higher than the epidermis (12–28 μm high). Cutaneous musculature thinner in the pre-pharyngeal region (mc:h 13% in the holotype) than in the anterior region of the body (mc:h 22% in the holotype), but gradually diminishing towards anterior tip.

Mesenchymal musculature (Fig. 4c–e) well developed, mainly composed of three layers: (1) dorsal subcutaneous, located mainly close to the cutaneous musculature, with decussate fibres (about 7–10 fibres thick); (2) supra-intestinal transverse (about 10–12 fibres thick); (3) sub-intestinal transverse (about 8–10 fibres thick). In addition, there are scattered ventral subcutaneous oblique fibres, as well as numerous dorso-ventral fibres. In the anterior region of the body, the mesenchymal musculature is less developed than in the pre-pharyngeal region (Fig. 4a).

Table 2 Body height and cutaneous musculature in the median region of a transversal section of the pre-pharyngeal region, in micrometres, and ratio of the height of cutaneous musculature to the height of the body (mc:h index) of specimens of *Matuxia tymbyra* Rossi & Leal-Zanchet, sp. nov.

	Holotype MZUSP PL.1563	Specimen MZU PL. 00180	Specimen MZU PL. 00182
Dorsal musculature	62	58	51
Ventral musculature	93	87	58
Dorsal epidermis	28	18	12
Ventral epidermis	31	25	20
Body height	1215	1054	868
Mc:h (%)	13	14	12.5
Creeping sole (%)	100	100	100

Pharynx

Pharynx cylindrical, about 1/20th of body length, with dorsal and ventral insertions about the same transversal level. Mouth at the end of the median third of pharyngeal pouch (Fig. 4f). Oesophagus with folded wall, with a length corresponding to 1/4th of the pharynx length. Oesophagus: pharynx ratio, 26% in the holotype.

Pharynx and pharyngeal lumen lined by ciliated cuboidal epithelium with insunk nuclei. Pharyngeal glands constituted by four secretory cell types: abundant secretory cells with fine granular xanthophil secretion and cells with amorphous cyanophil secretion, besides few cells with fine granular erythrophil secretion as well as cells with fine granular cyanophil secretion (Fig. 4f). Cell bodies of pharyngeal glands located in the mesenchyme, mainly anterior and laterally to pharynx.

Pharyngeal outer musculature (18–25 μm thick) comprised of thick subepithelial layer of longitudinal muscles, followed by a thicker circular layer. Circular layer becomes as thin as longitudinal one towards pharyngeal tip. Inner pharyngeal musculature (35–65 μm thick) comprises a thick circular subepithelial layer, followed by a thinner longitudinal layer. Inner and outer musculatures gradually become thinner towards pharyngeal tip.

The oesophagus is lined by cuboidal ciliated epithelium with insunk nuclei and coated with a thick circular subepithelial muscle layer, followed by a thinner longitudinal layer, (30–45 μm thick).

Reproductive organs

Testes in one irregular row on either side of the body, located beneath the dorsal transverse mesenchymal muscles (Fig. 4c–d). The follicles extend from the anterior fifth of the body, about at the same transverse level as the ovaries, to near to the root of the pharynx, in the median third of the body (Table 1). Sperm ducts dorsal to ovovitelline ducts in pre-pharyngeal region. They form spermiducal vesicles posteriorly to the pharynx. Distally, spermiducal vesicles enter the common muscular coat and bent dorso-anteriorly to open terminally into the forked portions of the prostatic vesicle (Fig. 5a–b). Intrabulbar prostatic vesicle composed of two portions, an unpaired and ovoid main portion and a proximal, tubular, forked portion that loops dorsally and posteriorly (Fig. 5a–b and 6a–d). The prostatic vesicle opens into the sinuous and folded ejaculatory cavity. The ample male atrium is occupied by a penis papilla, conical and asymmetrical, with dorsal insertion posteriorly displaced (Figs. 5a–b and 6a–b). Specimens MZU PL.00180 and MZU PL.00181 present part of prostatic vesicle within the papilla, probably due to contraction.

Prostatic vesicle lined with ciliated columnar to pseudostratified epithelium, receiving abundant fine granular erythrophil and amorphous cyanophil secretions (Fig. 6d). Muscularis of prostatic vesicle (20–30 μm thick) comprises interwoven longitudinal, oblique and circular fibres (Fig. 6c–d). Ejaculatory cavity lined with ciliated cuboidal epithelium, receiving numerous openings from glands with fine granular erythrophil and coarse granular xanthophil secretion, both with cell bodies internal to the common muscle coat. Muscle coat of ejaculatory cavity thick (12 μm–35 μm thick), comprised of subepithelial circular layer followed by a longitudinal layer.

The penis papilla is lined with non-ciliated columnar to cuboidal epithelium with irregular height. Penial glands with coarse granular xanthophil and fine granular erythrophil secretions as well as scarce cyanophil amorphous secretion. Cyanophil and xanthophil glands present cell bodies external to common muscle coat and necks running longitudinally in the papilla; erythrophil glands, intrapapillar cells bodies. Muscularis of the penis papilla (20–40 μm) mainly composed of circular fibres. Epithelial lining of male atrium columnar, non-ciliated, receiving openings from cyanophil glands with amorphous secretion. Muscularis of male atrium (5 μm–15 μm) comprised of thin circular subepithelial layer and a thicker subjacent longitudinal layer.

Vitelline follicles well developed in specimen MZU PL.00182 and inconspicuous in the holotype, as well as in specimen MZU PL.00180, situated between intestinal branches (Fig. 4c). Ovaries pyramidal and lobate, almost as long as wide, measuring about 0.35 mm in its antero-posterior axis and occupying one-third of the body height in the

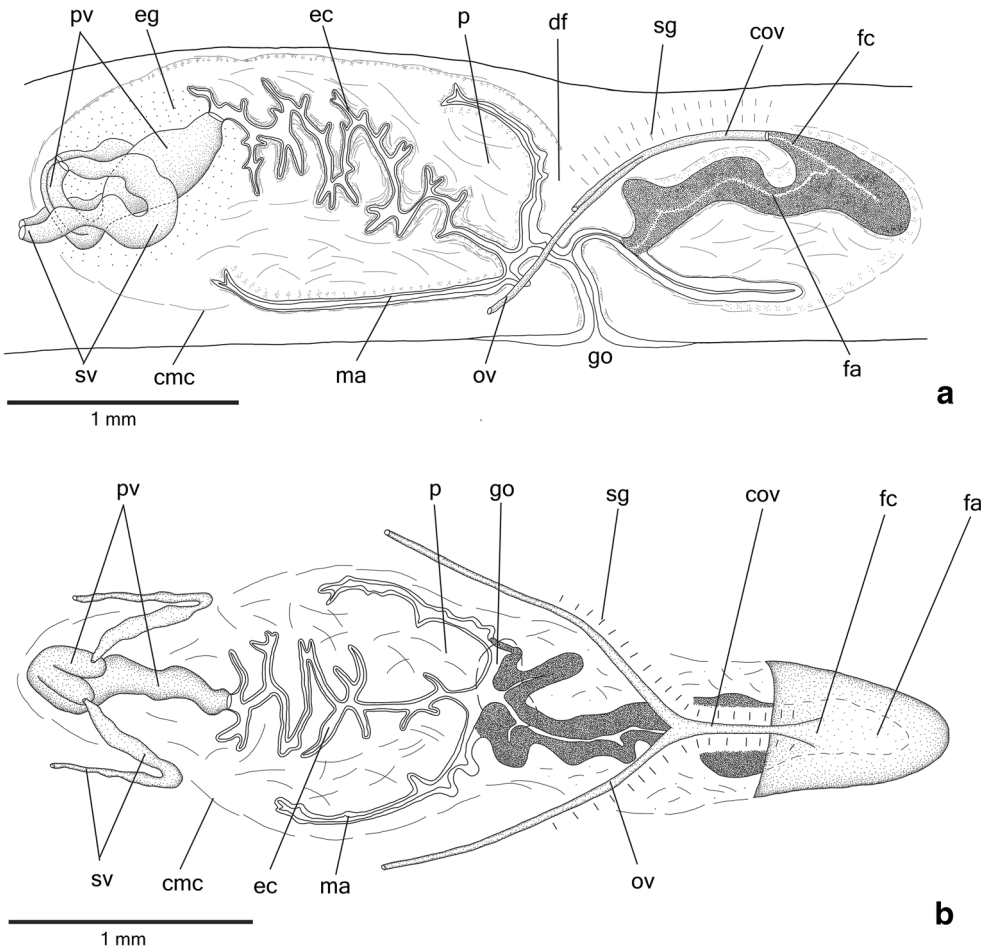

Fig. 5 *Matuxia tymbyra* Rossi & Leal-Zanchet, sp. nov.: **a** sagittal composite reconstruction of copulatory apparatus of the holotype; **b** horizontal composite reconstruction of copulatory apparatus of specimen MZU PL.00166

holotype (Fig. 4g). They are located immediately above the ventral nerve plate, about the same transversal level as the most-anterior testes (Table 1). Ovovitelline ducts emerge ventrally, but laterally displaced, from the anterior or median third of ovaries and run posteriorly immediately above the nerve plate. About at the gonopore level, ovovitelline ducts ascend posteriorly and medially inclined, to join dorsally to the distal or median third of female atrium, thus forming a long common glandular ovovitelline duct. Proximal portion of female atrium presents a dorso-anteriorly curved female canal (Figs. 5a–b and 6a). Female atrium ovoid with a pronounced proximal fold that projects distally and restricts the atrial cavity to an irregular gap (Figs. 5a and 6a). Length of female atrium 52%–118% of male atrium length (Table 1).

Ovovitelline ducts and common ovovitelline duct lined with ciliated, cuboidal to columnar epithelium, and covered with intermingled circular and longitudinal muscle fibres (3 μm – 12 μm thick). Numerous shell glands with xanthophil secretion empty into the common glandular ovovitelline duct, as well as into the distal ascending portion of paired ovovitelline ducts (Figs. 5a–b and 6a–b).

Female atrium lined mainly by a ciliated, tall epithelium exhibiting multilayered aspect (90 μm) (Fig. 6a, b, e), which becomes columnar in the roof of the female atrium. Female canal lined with ciliated, columnar to pseudostratified epithelium. Female atrium and canal receive numerous cyanophil amorphous secretion and finely granular, erythrophil secretion. Muscularis of female canal and atrium (20 μm–35 μm thick) composed of circular fibres mixed with scarce longitudinal fibres.

Male and female atria separated by a large dorsal fold (Figs. 5a and 6a). Gonopore canal vertical at the sagittal plane, lined with ciliated, columnar epithelium, receiving the abundant openings of glands containing amorphous cyanophil secretion, as well as glands with coarse granular xanthophil secretion, and scarcer glands with finely granular erythrophil secretion. Muscularis of gonopore canal comprised of circular subepithelial fibres and subjacent longitudinal fibres.

Male and female atria with continuous muscle coat, consisting of circular, longitudinal and oblique fibres. A stroma with sparse mixed muscle fibres separates the atrial muscularis and common muscle coat.

Comparative discussion

In accordance with the phylogenetic analyses, the assignment of the new species herein described to the genus *Matuxia* Carbayo

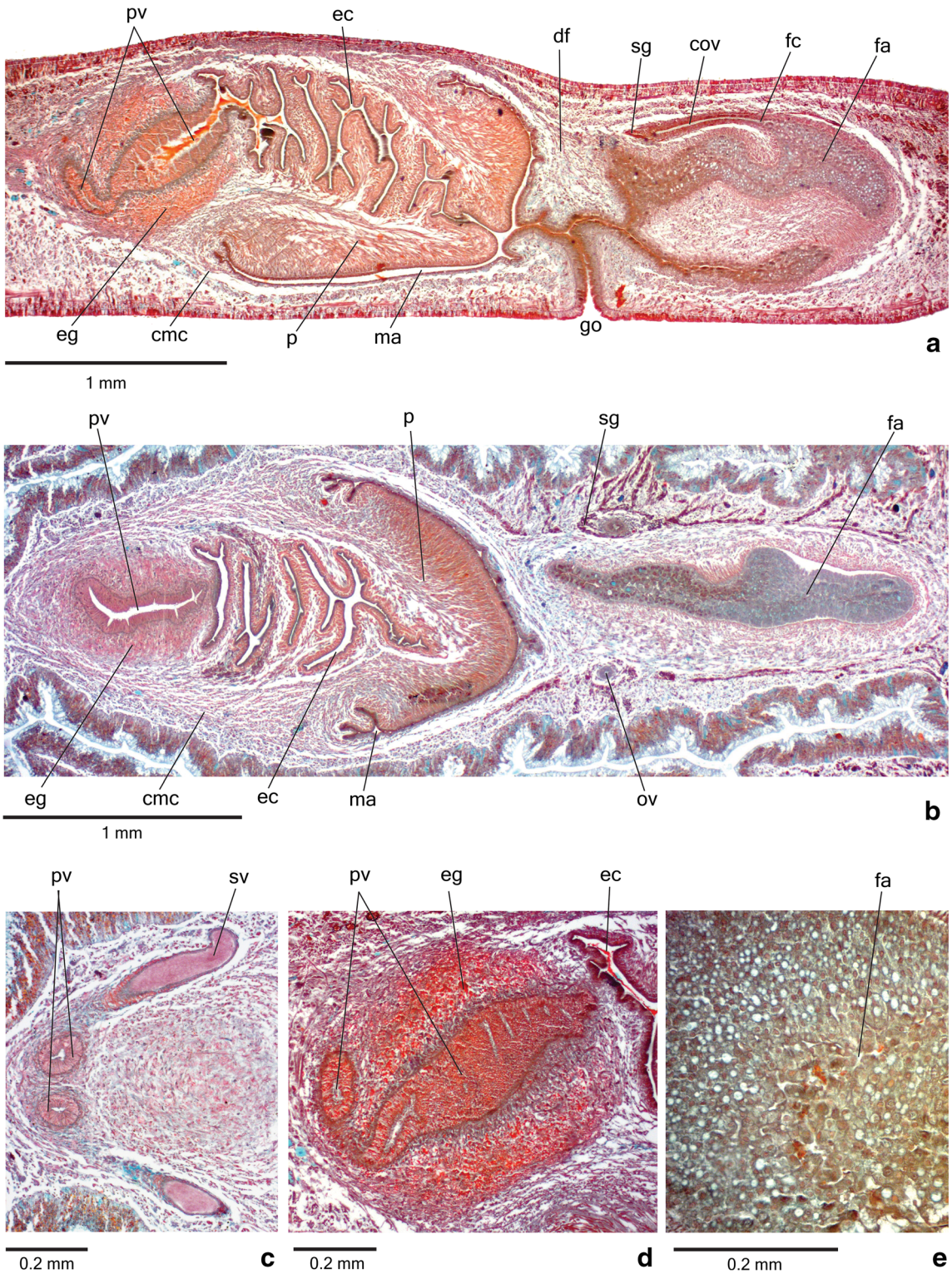

Fig. 6 *Matuxia tymbyra* Rossi & Leal-Zanchet, sp. nov., microphotographs of the copulatory apparatus: **a** holotype in sagittal section; **b** MZU PL.00166 in horizontal section; **c** detail of prostatic vesicle of specimen MZU PL.00166 in horizontal section; **d** detail of prostatic vesicle of holotype in sagittal section; **e** detail of female atrium of holotype in sagittal section

et al. (2013) is supported by characters of the external morphology, namely body margins nearly parallel and monolobated eyes, and internal characteristics, such as the shape of the male copulatory organ and the ejaculatory cavity and the anatomy and histology of the female atrium.

In respect of external features, *Matuxia tymbyra* Rossi and Leal-Zanchet, sp. nov. differs from *M. matuta* by the body length and the dorsal colour of the body. The only known specimen of *M. matuta*, with 120 mm of body length (Froehlich 1955b), is larger than mature specimens of *M. tymbyra*, the body length of which varies from 65 to 88 mm. In addition, *M. matuta* has the dorsal surface of the body covered by a reddish reticular pigmentation and brown small spots in a median zone (Froehlich 1955b), whereas in *M. tymbyra* there is a thin and densely distributed dark-grey pigmentation except on a thin median stripe and body margins. Mature specimens of *M. tuxaua*, with body length varying from 45 to 65 mm (Froehlich 1955b), are smaller than mature specimens of *M. tymbyra*. The general dorsal colour pattern of *M. tymbyra* is similar to that described and illustrated by Froehlich (1955b) for *M. tuxaua*.

Regarding anatomical features, both species formerly included within *Matuxia* as well as *M. tymbyra* show a similar copulatory apparatus. *Matuxia tymbyra* differs from *M. matuta* by the way that the sperm ducts approach the forked portion of the prostatic vesicle. They run upwards inside the penis bulb and open into the forked portion of the prostatic vesicle of *M. matuta*. In contrast, in *M. tymbyra*, the sperm ducts run posteriorly inside the penis bulb and loop anteriorly to open into the forked portions of the vesicle, similarly to the situation in *M. tuxaua*. The shape of the penis papilla of *M. tymbyra* resembles that of *M. tuxaua*, showing the dorsal insertion posteriorly displaced, whereas in *M. matuta*, both insertions are at almost the same transversal level (Froehlich 1955b). *Matuxia tymbyra* also differs from *M. matuta* by the morphology of the female atrium that is unfolded and shows a non-ciliated, high epithelium lining almost the whole length of the female atrium. In *M. tymbyra*, similarly to *M. tuxaua*, the female atrium is folded and its epithelial lining is ciliated and lower compared to that of *M. matuta*.

In conclusion, regarding external and internal characters, *M. tymbyra* and *M. tuxaua* seem to be sibling species. The phylogenetic analyses, the delimitation approaches GMYC and PTP, as well as molecular autapomorphies point to the close relationship between these species, supporting them as evolutionary independent molecular operational taxonomic units (MOTUs).

General discussion

Knowledge concerning the geographic and genetic divergence within the genus *Matuxia*, proposed by Carbayo et al. (2013) for two species occurring in nearby areas of southeast Brazil, is herein enhanced and its monophyly confirmed. We describe a southern lineage for the genus, which is almost indistinguishable, based on anatomical and histological features, from the type-species of the genus, *M. tuxaua*. Molecular analyses indicate a close relationship between *M. tuxaua* and *M. tymbyra*, which may constitute sibling species. Another species from southeast Brazil, *M. matuta*, represents the most basal species. The present discontinuous distribution of the genus, without specimens occurring in the states of Santa Catarina and Paraná, is possibly a result of the absence of extensive land flatworm samplings in these areas.

The recognition of *M. tymbyra* as a new species was indicated by both species delimiters (GMYC and PTP) used herein with the dataset including the two concatenated genes, and supported by molecular autapomorphies inferred for the COI and EF-1a genes. We recorded 97 molecular autapomorphies; 79 for the mitochondrial gene and 18 for the nuclear gene. Considering the two genes, *M. tymbyra* sp. nov. is supported as a new species for the genus by presenting 18 autapomorphies. Finally, it should be noted that mean interspecific distance between *M. tymbyra* sp. nov. and the other species of the genus was 7.3% (*M. tuxaua*) and 11.5% (*M. matuta*). In different integrative taxonomy studies, it has been found that genetic distances above 6% (Rossi et al. 2015; Amaral et al. 2018a,b; Carbayo et al. 2017; Marques et al. 2018) indicate the existence of evolutionary independent molecular operational taxonomic units (MOTUs).

The near absence of anatomical and histological differences between *M. tuxaua* and *M. tymbyra* may be due to their close relationship. However, details of the histology of the epidermis, relative position of ovaries and testes, shape of the ovaries and position of the opening of the ovovitelline ducts into the ovaries, as well as the histology of the copulatory apparatus could provide other characters to differentiate both species, but the literature presents no reference for them regarding *M. tuxaua*. Such characters were useful to distinguish species in other Geoplaninae genera (Leal-Zanchet and Froehlich 2006; Amaral et al. 2012, 2018b; Rossi & Leal-Zanchet 2017; Marques et al. 2018).

Acknowledgements We gratefully acknowledge the Conselho Nacional de Desenvolvimento Científico Tecnológico — CNPq (research grants 167467/2017-4 and 308996/2017-8) and the Coordenação de Aperfeiçoamento de Pessoal de Nível Superior - CAPES for research grants and fellowships in support of this study. We thank the Instituto Chico Mendes de Conservação da Biodiversidade for collection licence permits (SISBIO 24357-1). We are indebted to Dr. V. Baptista, Dr. P. Boll, Biol. L. Teixeira and Dr. N. Zanchet for their help during field works, Biol. L. Teixeira for her help in section preparation, MSc. E. Benya for an English review of the manuscript and Dr. P. Boll for suggestions regarding the species name. We appreciated the constructive comments and suggestions by Dr. L. Negrete and an anonymous reviewer on an early version of the manuscript.

Data availability The datasets generated during the current study are available in the TreeBASE repository, http://purl.org/phylo/treebase/phylows/study/TB2:S24493

References

Akaike, H. (1974). A new look at the statistical model identification. *IEEE Transactions on Automatic Control, 199*(6), 716–723. https://doi.org/10.1109/TAC.1974.1100705.

Álvarez-Presas, M., Carbayo, F., Rozas, J., & Riutort, M. (2011). Land planarians (Platyhelminthes) as a model organism for fine-scale phylogeographic studies: understanding patterns of biodiversity in the

Brazilian Atlantic Forest hotspot. *Journal of Evolutionary Biology, 24, 24*(4), 887–896. https://doi.org/10.1111/j.1420-9101.2010.02220.x.

Álvarez-Presas, M., Amaral, S. V., Carbayo, F., Leal-Zanchet, A. M., & Riutort, M.(2015) Focus on the details: morphological evidence supports new cryptic land flatworm (Platyhelminthes) species revealed with molecules. *Organisms Diversity & Evolution*, *15*(2), 379–403. https://doi.org/10.1007/s13127-014-0197-z

Amaral, S. V., Oliveira, S. M., & Leal-Zanchet, A. M. (2012). Three new species of land flatworms and comments on a complex of species in the genus *Geoplana* Stimpson (Platyhelminthes: Continenticola). *Zootaxa, 3338*, 1–32. https://doi.org/10.5281/zenodo.281355.

Amaral, S. V., Ribeiro, G. G., Müller, M. J., Valiati, V. H., & Leal-Zanchet, A. M. (2018a). Tracking the diversity of the flatworm genus *Imbira* (Platyhelminthes) in the Atlantic Forest. *Organisms Diversity & Evolution, 18*, 87–99. https://doi.org/10.1007/s13127-018-0358-6.

Amaral, S. V., Ribeiro, G. G., Valiati, V. H., & Leal-Zanchet, A. M. (2018b). Body doubles: an integrative taxonomic approach reveals new sibling species of land planarians. *Invertebrate Systematics, 32*(3), 533–550. https://doi.org/10.1071/IS17046.

Bickford, D., Lohman, D. J., Sodhi, N. S., Ng, P. K. L., Meier, R., Winker, K., Ingram, K. K., & Das, I. (2007). Cryptic species as a window on diversity and conservation. *TRENDS in Ecology and Evolution, 22*(3), 148–155. https://doi.org/10.1016/j.tree.2006.11.004.

Bouckaert, R., Heled, J., Kühnert, D., Vaughan, T., Wu, C., Xie, D., Suchard, M. A., Rambaut, A., & Drummond, A. J. (2014). BEAST 2: a software platform for Bayesian evolutionary analysis. *PLoS Computational Biology, 10*(4), e1003537. https://doi.org/10.1371/journal.pcbi.1003537.

Carbayo, F., Alvarez-Presas, M., Olivares, C. T., Marques, F. P. L., Froehlich, E. M., & Riutort, M. (2013). Molecular phylogeny of Geoplaninae (Platyhelminthes) challenges current classification: proposal of taxonomic actions. *Zoologica Scripta, 42*(5), 508–528. https://doi.org/10.1111/zsc.12019.

Carbayo, F., Silva, M. S., Riutort, M., & Alvarez-Presas. (2017). Rolling into the deep of the land planarian genus *Choeradoplana* (Tricladida, Continenticola, Geoplanidae) taxonomy. *Organisms Diversity & Evolution, 18*(2), 187–210. https://doi.org/10.1007/s13127-017-0352-4.

Darriba, D., Taboada, G. L., Doallo, R., & Posada, D. (2012). jModelTest 2: more models, new heuristics and highperformance computing. *Nature Methods, 9*(8), 772. https://doi.org/10.1038/nmeth.2109.

Felsenstein, J. (1985). Confidence limits on phylogenies: an approach using the bootstrap. *Evolution, 39*, 791–793.

Frankham, R., Ballou, J. D., Dudash, M. R., Eldridge, M. D. B., Fenster, C. B., Lacy, R. C., Mendelson, J. R. III, Porton, I. J., Ralls K., & Ryder O. A. (2012) Implications of different species concepts for conserving biodiversity. *Biological Conservation*, *153*, 25–31. https://doi.org/10.1016/j.biocon.2012.04.034.

Froehlich, C. G. (1955a). Sobre a morfologia e taxonomia das Geoplanidae. *Boletim da Faculdade de Filosofia, Ciências e Letras da Universidade de São Paulo, Série. Zoologia, 19*, 195–279.

Froehlich, E. M. (1955b). Sobre espécies brasileiras do gênero *Geoplana*. *Boletim da Faculdade de Filosofia, Ciências e Letras da Universidade de São Paulo, Série. Zoologia, 19*, 289–369.

Fujisawa, T., & Barraclough, T. G. (2013). Delimiting species using single-locus data and the generalized mixed yule coalescent approach: a revised method and evaluation on simulated data sets. *Systematic Biology, 62*(5), 707–724.

Hall, T. A. (1999). BioEdit: a user-friendly biological sequences alignment editor and analysis program for Windows 95/98 NT. *Nucleid Acids Symposium Serie, 41*, 95–98.

Hillis, D. M., & Bull, J. J. (1993). An empirical test of bootstrapping as a method for assessing confidence in phylogenetic analysis. *Systematic Biology, 42*(2), 182–192. https://doi.org/10.1093/sysbio/42.2.182.

Kimura, M. (1980). A simple method for estimating evolutionary rates of base substitutions through comparative studies of nucleotide sequences. *Journal of Molecular Evolution, 16*(2), 111–120. https://doi.org/10.1007/BF01731581.

Lázaro, E. M., Sluys, R., Pala, M., Stocchino, G. A., Baguñà, J., & Riutort, M. (2009). Molecular barcoding and phylogeography of sexual and asexual freshwater planarians of the genus Dugesia in the Western Mediterranean (Platyhelminthes, Tricladida, Dugesiidae). *Molecular Phylogenetics and Evolution, 52*(3), 835–845. https://doi.org/10.1016/j.ympev.2009.04.022.

Leal-Zanchet, A. M., & Baptista, V. A. (2009). Planárias terrestres (Platyhelminthes: Tricladida) em áreas de floresta com Araucária no Rio Grande do Sul. In C. R. S. Fonseca, A. F. Souza, T. L. Dutra, A. M. Leal-Zanchet, A. Backes, & G. M. S. Ganade (Eds.), *Floresta com Araucária: Ecologia, Conservação e Desenvolvimento Sustentável* (pp. 199–207). Ribeirão Preto: Holos.

Leal-Zanchet, A. M., & Carbayo, F. (2000). Fauna de planárias terrestres da Floresta Nacional de São Francisco de Paula, RS, Brasil: uma análise preliminar. *Acta Biologica Leopoldensia, 22*, 19–25.

Leal-Zanchet, A. M., & Froehlich, E. M. (2006). A species complex in the genus *Notogynaphallia* Ogren and Kawakatsu (Platyhelminthes: Tricladida: Terricola) with a taxonomic revision of homonyms of *Geoplana marginata* Schultze & Müller and a reinterpretation of *Notogynaphallia caissara* (Froehlich) anatomy. *Belgian Journal of Zoology, 136*(1), 81–100.

Leal-Zanchet, A. M., Baptista, V. A., Campos, L. M., & Raffo, J. F. (2011). Spatial and temporal patterns of land flatworm assemblages in Brazilian Araucaria forests. *Invertebrate Biology, 130*(1), 25–33. https://doi.org/10.1111/j.1744-7410.2010.00215.x.

Lemos, V. S., Cauduro, G. P., Valiati, V. H., & Leal-Zanchet, A. M. (2014). Phylogenetic relationships within the flatworm genus *Choeradoplana* Graff (Platyhelminthes: Tricladida) inferred from molecular data with the description of two new sympatric species from Araucaria moist forests. *Invertebrate Systematics, 28*, 605–627.

Marques, A., Rossi, I., Valiati, V. H., & Leal-Zanchet, A. M. (2018). Integrative approach reveals two new species of *Obama* (Plateyhelminthes: Tricladida) from the South-Brazilian Atlantic Forest. *Zootaxa, 4455*(1), 099–126. https://doi.org/10.11646/zootaxa.4455.1.4.

Monaghan, J. R., Epp, L. G., Putta, S., Page, R. B., Walker, J. A., Beachy, C. K., Zhu, W., Pao, G. M., Verma, I. M., Hunter, T., Bryant, S. V., Gardiner, D. M., Harkins, T. T., & Voss, S. R. (2009). Microarray and cDNA sequence analysis of transcription during nerve-dependent limb regeneration. *BMC Biology, 7*, 1. https://doi.org/10.1186/1741-7007-7-1.

Pons, J., Barraclough, T. G., Gomez-Zurita, J., Cardoso, A., Duran, D. P., Hazell, S., Kamoun, S., Sumlin, W. D., & Vogler, A. P. (2006). Sequence-based species delimitation for the DNA taxonomy of undescribed insects. *Systematic Biology, 55*(4), 595–609. https://doi.org/10.1080/10635150600852011.

Rambaut, A., & Drummond, A.J. (2009). Tracer version 1.5. http://beast.bio.ed.ac.uk

Romeis, B. (1989). *Mikroskopische Technik*. München: Urban und Schwarzenberg.

Ronquist, F., Teslenko, M., van der Mark, P., Ayres, D. L., Darling, A., Höhna, S., Larget, B., Liu, L., Suchard, M. A., & Huelsenbeck, J. P. (2012). MrBayes 3.2: efficient Bayesian phylogenetic inference and model choice across a large model space. *Systematic Biology, 61*(3), 539–542. https://doi.org/10.1093/sysbio/sys029.

Rossi, I., & Leal-Zanchet, A. M. (2017). Three new species of *Cratera* Carbayo et al., 2013 from *Araucaria* forests with a key to species of the genus (Platyhelminthes, Continenticola). *ZooKeys, 643*, 1–32. https://doi.org/10.3897/zookeys.643.11093.

Rossi, I., Amaral, S. V., Ribeiro, G. G., Cauduro, G. P., Fick, I., Valiati, V. H., & Leal-Zanchet, A. M. (2015). Two new Geoplaninae species (Platyhelminthes: Continenticola) from Southern Brazil based on an integrative taxonomic approach. *Journal of Natural History, 50*, 1–29. https://doi.org/10.1080/00222933.2015.1084057.

Saez, A. G., & Lozano, E. (2005). Body doubles. *Nature, 433*, 111. https://doi.org/10.1038/433111a.

Stamatakis, A. (2006). RAxML-VI-HPC: maximum likelihood-based phylogenetic analyses with thousands of taxa and mixed models. *Bioinformatics, 22*(21), 2688–2690. https://doi.org/10.1093/bioinformatics/btl446.

Swofford, D. L. (2002). PAUP*. Phylogenetic analysis using parsimony (*and other methods). Version 4.0b10. Sinauer associates, Sunderland, M.A, USA. https://doi.org/10.1111/j.0014-3820.2002.tb00191.x.

Tamura, K., Stecher, G., Peterson, D., Filipski, A., & Kumar, S. (2013). MEGA6: molecular evolutionary genetics analysis version 6.0. *Molecular Biology and Evolution, 30*, 2725–2729. https://doi.org/10.1093/molbev/mst197.

Thompson, J. D., Gibson, T. J., Plewniak, F., Jeanmougin, F., & Higgins, D. G. (1997). The CLUSTAL_X windows interface: flexible strategies for multiple sequence alignment aided by quality analysis tools. *Nucleic Acids Research, 25*(24), 4876–4882.

Zhang, J., Kapli, P., Pavlidis, P., & Stamatakis, A. (2013). A general species delimitation method with applications to phylogenetic placements. *Bioinformatics, 29*(22), 2869–2876. https://doi.org/10.1093/bioinformatics/btt499.